Temperature effects on energy production by salinity exchange

Silvia Ahualli, María M. Fernández, Guillermo Iglesias, Ángel V. Delgado, and María L. Jiménez*

*Department of Applied Physics, School of Sciences, University of Granada, 18071, Granada, Spain.*

E-mail: jimenezo@ugr.es

Phone: +34 958 241000 Ext. 20389. Fax: +34 958 243214

Abstract

In recent years, the capacitance of the interface between charged electrodes and ionic solutions (the electric double layer) has been investigated as a source of clean energy. Charge is placed on the electrodes either by means of ion-exchange membranes or of an external power source. In the latter method, net energy is produced by simple solution exchange in open circuit, due to the associated decrease in the capacitance of the electric double layer. In this work, we consider the change in capacitance associated to temperature variations: the former decreases when temperature is raised, and hence, a cycle is possible in which some charge is put on the electrode at a certain potential and returned at a higher one. We demonstrate experimentally that it is thus viable to obtain energy from electric double layers if these are successively contacted with water at different temperatures. In addition, we show theoretically and experimentally that temperature and salinity variations can be conveniently combined to maximize the electrode potential increase. The resulting available energy is also estimated.

---

*To whom correspondence should be addressed

TOC Art

2
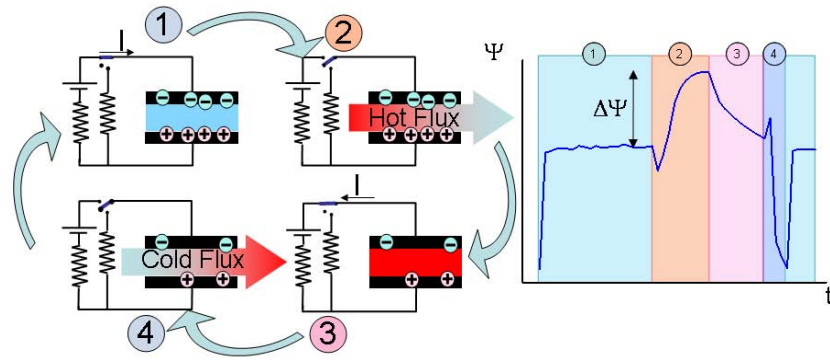
Introduction

There are many industrial processes where water is used as coolant, and returned to the cold water reservoir, so that a mixture is produced of hot and cold fluids. The temperature gradient between them can be quite high in the case of thermal power plants, where heat transfer from hot to cold reservoirs is the most widely exploited route for producing electrical energy, but whatever the process where refrigeration is required, exergy is wasted by simply mixing the two kinds of water. Although temperature differences between the water input and output are hardly above 20 °C, after being refrigerated in the power plant, waters near geysers or thermal waters in volcanic areas can reach 85 °C or more.

In this paper we propose taking advantage of solution temperature differences in the direct production of electrical energy. This can be done by properly using the capacitance changes induced in microporous electrodes by exchanging solutions in contact with them with alternatively high and low salt concentrations. Such exchange modifies the capacitance of the electrical double layer, that is, the interface between the charged electrode surface and the solution.[1–3] Energy production by this capacitance modification is known as Capacitive energy extraction based on Double Layer Expansion (CDLE) and it is enclosed in the group of emergent technologies jointly known as Capmix methods.[2–4] These are all based on the change of the electrical properties of the electrode-solution interface associated to salinity variations.

Inspired in such phenomenology, the idea emerges of exploiting the above mentioned process in conditions where the capacitance of the electric double layer (EDL) is modified by an additional mechanism. This is to use the temperature gradients that are generated in rivers when their water is used in industrial processes, even if such water is only used for refrigeration and no contamination other than thermal one takes place. Additionally, the mixture of hot river water and cold sea water (as in the mouth of a river coming into a much colder ocean, mostly if the river water has been previously employed in the refrigeration of power plants) may be advantageous as well, by adding the effect of temperature changes to

that of ionic contents differences.

Exploiting the temperature effect on energy production systems is an idea present in other techniques. For instance, Sales[5] has recently proposed to use the so-called *thermal membrane potential*: an electric potential is generated when hot and cold waters are contacted with anion and cation exchange membranes, respectively. That potential can be used in energy production by charging carbon electrodes in contact with the membranes, and discharging them through the external circuit. This is a modification of the capacitive mixing procedure known as CDP (Capacitive energy extraction based on Donnan Potential), also a member of the Capmix family.[3,4,6]

In this work, we show some results concerning the implementation of CDLE with temperature differences between the two solutions used in the exchange process. A theoretical model based on cylindrical geometry for the electrode micropores is described and its predictions discussed. Experimental results are also offered, and their agreement (at least qualitative) with the theoretical description is analyzed.

Principles of the method

We begin by considering two charged electrodes in contact with salty water. Ions in solution migrate towards the electrode of opposite sign, and some charge accumulates at the electrode solution interface, forming the EDL.[7] Below 1 V, faradaic reactions can be excluded, and hence, electrodes are charge blocking, meaning that positive and negative charges are separated at the interface, which in fact behaves as a capacitor.[8] Due to diffusion, the EDL extends over a finite thickness, and the surface charge density σ and surface potential Ψ_S can be, to a first approximation, related by[9]

$$\sigma = \sqrt{8\varepsilon_m(T)\varepsilon_0 n k_B T}\sinh\frac{ze\Psi_S}{2k_B T} \tag{1}$$

$_{67}$ where $\varepsilon_m\varepsilon_0$ is the permittivity of the solution, k_B is the Boltzmann constant, T the absolute

$_{68}$ temperature, an aqueous solution of a symmetric z-valent electrolyte with number concen-

$_{69}$ tration n of each ion, is assumed, and e is the electron charge. In the CDLE process, a

$_{70}$ change in the capacitance of the EDL is produced by changing the salinity of the solution

$_{71}$ in contact with the interface: a decrease in n at constant σ produces a higher potential Ψ_S

$_{72}$ (eq 1).

$_{73}$ Additionally, modifications can be produced by changing the permittivity of the solution,

$_{74}$ by, for instance, increasing or reducing its temperature. Specifically, an increase in tempera-

$_{75}$ ture produces a decrease of the electric permittivity of water, and, as a consequence, a larger

$_{76}$ electrode potential for given charge. In fact, from eq 1, it can be easily obtained that the

$_{77}$ differential capacitance

$$C_d = \frac{\mathrm{d}\sigma}{\mathrm{d}\Psi_S} = ze\sqrt{\frac{\sigma^2}{4k_B^2T^2} + \frac{2\varepsilon_0\varepsilon_m(T)n}{k_BT}} \tag{2}$$

$_{78}$ decreases with temperature, if ε_m does.

$_{79}$ In Figures 1, 2, we present a cycle designed for obtaining electric energy from tempera-

$_{80}$ ture differences. Because in this case there are no salinity differences between the solutions

$_{81}$ used, but just temperature variations, we propose to denominate DLPE (or *Double Layer*

$_{82}$ *Permittivity Exchange*) to the technique. At the first stage the electrodes are externally

$_{83}$ connected to a battery with potential difference V in the presence of cold water. At equi-

$_{84}$ librium, the same potential difference will be established between both electrodes. Each of

$_{85}$ them will acquire a surface charge equal to σ_A in absolute value, and a potential difference

$_{86}$ $|\Psi_0| = |V|/2$ with respect to the solution in the space between them (1 in Figures 1, 2).

$_{87}$ Then, in open circuit, cold and hot waters are interchanged (step 1→2 in Figure 1, 2). As

$_{88}$ a consequence of the temperature increase, the permittivity decreases and so does the EDL

$_{89}$ capacitance. Since the circuit is open, this provokes an increase of the electric potential to

$_{90}$ Ψ_H at the electrode-solution interface, as can be seen in Figure 2. In order to take advantage

$_{91}$ of this increase in potential, we next discharge the electrodes (step 2→3) over the external

source. Since the potential of the electrodes is larger, some charge will spontaneously migrate to the battery at a larger potential, as observed in Figure 2, resulting in a positive energy balance. A new equilibrium is attained, and the potential returns to the initial value but with a difference surface charge σ_B. For closing the cycle, we next exchange hot by cold water in open circuit (step 3→4) and this leads to a decrease of the potential below that of the external battery to Ψ_L. Finally, we connect again the battery to the cell filled with cold water (step 4→1) and return to the initial potential and charge density values.
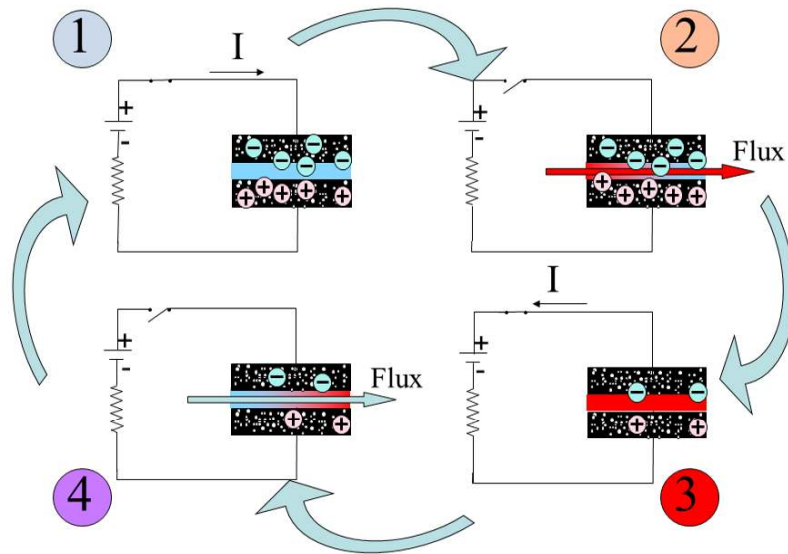
Figure 1: Cell during every step of the cycle (1: cell charged in cold water; 2: hot water in. 3: electrode discharge. 4: cold water in.)

Theoretical model

In order to increase the charge transfer in step 2→3 of Figure 2, electrodes made of microporous carbon particles can be used because of their huge surface area. However, since the charging potential can be relatively high (several hundred mV) and the pore diameter can be as low as 1 nm, simple models assuming low potentials and planar interfaces may not describe accurately the phenomenon. Furthermore, the behavior of the ions close to
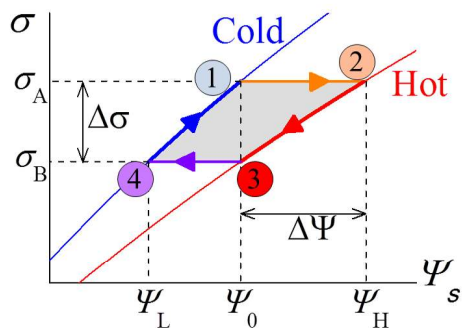
Figure 2: Schematic electrode charge vs. electrode potential relation for cold and hot waters. The DLPE cycle is enlighted with arrows.

the wall is another source of difficulty, as they can even lose their hydration shell (fully or in part) under the EDL field. This is the case of ionic liquids,[10,11] and is the basis of the supercapacitances that are found with activated carbons with pores of size below 1 nm, but can happen even for small, monovalent, well hydrated ions like Na^+, as has been shown by molecular dynamics simulations.[12] As a consequence, a Stern layer can be formed with ions located between the inner and outer Helmholtz planes, which are partially dehydrated due to strong chemical or electric interactions with the surface. However, there is no evidence of such strongly adsorbed ions at the carbon-sodium chloride interface, and in our model the traditional image of a charge-free Stern layer determined by the distance of minimum approach of hydrated Na^+ and Cl^- ions will be considered.

We will focus on the modeling of the solution-pore wall interface inside the porous material, which is of course just part of the description of the complete electrode. Also, as in other analyses of the electrochemistry of porous electrodes, time effects will be ignored and only steady state situations will be considered (a model including a kinetic analysis of the electrode response has been described recently by Rica et al.[13,14]). For our purposes, an equilibrium description of every stage of the cycle will be enough for predicting the electrical energy that can be potentially extracted with this method.

Existing models on the description of the EDL potential profile at interfaces with different

7

geometries[7,15–22] cannot be applied to porous electrodes because such models are usually restricted to dilute suspensions, so that the likely overlap between EDLs from opposite walls of the pores is not considered. Theoretical models including EDL overlap and ionic size effects have been applied to salt free suspensions,[19] and are based on cell models, which are appropriate in the case of homogeneous distributions of non-contacting spherical particles.[18]

In this work, we propose an approach in which the porous electrodes are modelled as a swarm of cylindrical pores. We will include the following aspects in our simulations:

- Non-Planar EDL: inside the activated particles, the most abundant pores are typically less than 5 nm in diameter, and curvature effects on the electric potential profile can be significant.

- EDL overlap: it is likely in the smallest pores and with the less concentrated solutions, considering that the potentials used for charging can be relatively high.

- Moderate charging potentials: larger energies can in principle be obtained if large amounts of charge are transferred back and forth at very different potentials. For fixed values of the salinity, it may be necessary to explore potential differences as high as 500-600 mV. In such conditions, the interfacial region can be largely enriched in counterions, to the extent that the point charge hypothesis for EDL structure leads to unrealistically high counterion concentrations in the vicinity of the pore wall. This fact, together with the high salinity of the sea water, means a non-negligible role of the size of the ions.

This model is an extension to cylindrical pores of the one presented in.[23] Since the most abundant ions in natural waters are Na^+ and Cl^- we will restrict the analysis to this salt, although a more general solution composition can be considered if needed. Hence, we perform a mean field analysis of the structure of the EDL, and so, the electric potential distribution

will be given by Poisson's equation:

$$\nabla^2 \Psi(\mathbf{r}) = \frac{1}{r}\frac{\partial}{\partial r}\left(r\frac{\partial \Psi(r)}{\partial r}\right) = -\frac{ez\left(n^+(r) - n^-(r)\right)}{\varepsilon_0 \varepsilon_m(T)} \tag{3}$$

In this equation, Ψ is the electrostatic potential at position $\mathbf{r}$, r is the cylindrical radial coordinate with origin at the pore axis, e the electron charge, and n^+ (n^-) is the number concentration of cations (anions) at the specified position. The temperature dependence of the electric permittivity of the solvent is implicitly indicated. For this work, the permittivity values of Table 1 were used at every temperature.

Table 1: Relative permittivity of water for different temperatures

T(°C)	ε_m	T(°C)	ε_m
15	82.2	50	69.9
20	80.4	55	68.3
25	78.5	65	65.2
35	75.0	80	60.8
45	71.6		

This equation will be solved subject to the following boundary conditions (r is the radial cylindrical coordinate with origin at the pore axis), specifying the surface potential of the pore wall, Ψ_S, and the zero electric field at the pore axis:

$$\Psi(r = R) = \Psi_S \tag{4}$$

$$\left.\frac{d\Psi}{dr}\right|_{r=0} = 0 \tag{5}$$

The interaction between ions can be taken into account by using sophisticated models as described in Refs.[17,24,25] These models consider both coulombic and excluded volume interactions between every pair of ions instead of using a mean field approximation. They provide a detailed profile of the electric potential and predict interesting effects like charge inversion.[17] However, we are not interested in such precise profile, but rather in the effect

of the finite volume of ions on the total stored charge in the EDL. An extensive analysis of the different approximations is given in[15,26] and some consequences on the differential capacitance of the EDL are studied in.[27]

For the present approach, the relation between the ionic concentration and the electric potential at any point is based on the approximation provided in[18,28,29] which takes into account the excluded volume of ions:

$$n^{\pm}(r) = \frac{n^{\pm}_{\infty} \exp\left[\mp \frac{ze\Psi(r)}{k_B T}\right]}{1 + \frac{n^+_{\infty}}{n^+_{MAX}}\left[\exp\left(-\frac{ze\Psi(r)}{k_B T}\right)\right] + \frac{n^-_{\infty}}{n^-_{MAX}}\left[\exp\left(\frac{ze\Psi(r)}{k_B T}\right)\right]} \tag{6}$$

where $n^{\pm}_{\infty}$ and $n^{\pm}_{MAX}$ denote, respectively, the bulk concentration and the maximum concentration allowed for the corresponding ionic species.

Note that we also take into account the excluded volume between particle surface and hydrated ions. Hence, Eq. 3 must be solved separately in different regions. In the first one, between the particle surface and the radius of the smallest ion (Cl^- in the case of NaCl), $n^{\pm}(r) = 0$. In the second region, where only the smallest ion can stay, we can write $n^+(r) = 0$. In the third region all ions can stay and hence, no restriction is imposed on ionic concentration. Accordingly, new boundary conditions must be used, namely, the continuity of the potential and of the normal component of the electric displacement at the boundary between every pair of regions:

$$\Psi(r = R - r^-_{Cl,Na}) = \Psi(r = R - r^+_{Cl,Na}) \tag{7}$$

$$\left.\frac{d\Psi}{dr}\right|_{r=R-r^-_{Cl,Na}} = \left.\frac{d\Psi}{dr}\right|_{r=R-r^+_{Cl,Na}} \tag{8}$$

Note that the existence of a minimum distance of approach of ions to the pore wall (with thickness controlled by the ion radius) determines a charge-free inner layer at the edge of the diffuse layer. This was first hypothesized by Stern and has become an essential component of

the classical electrochemistry of EDLs.[15,30] This *Stern layer* is often modelled by a constant capacitance C^i, which is responsible for a significant part of the voltage drop when the diffuse layer capacitance grows to very high values (high electrolyte concentrations).

With the previous equations, the potential profile can be calculated as a function of surface potential, pore size, ionic concentration, and, in our case, temperature. The surface charge density, σ, is:[9]

$$\sigma = -\varepsilon_0 \varepsilon_m(T) \frac{\mathrm{d}\Psi}{\mathrm{d}r}\bigg|_{r=R} \tag{9}$$

Finally, the extracted work in every cycle is represented by twice the shadowed area in Figure 2 (one term for each electrode):

$$W_S = 2 \int_{\sigma_B}^{\sigma_A} \big[\Psi_S(\text{hot}) - \Psi_S(\text{cold})\big] \mathrm{d}\sigma \tag{10}$$

Roughly speaking, the area is $2\Delta\sigma\Delta\Psi$. This is important to be stated, because from this it is clear that the extracted work can be increased by increasing either the charge exchanged $\Delta\sigma$, the potential rise $\Delta\Psi$, or both. It must be emphasized that all calculations presented in the work were performed using the model described.

Materials and Methods

In Figure 3 we present a scheme and a picture of the cell. The two electrodes are composed by a graphite current collector on which activated carbon particles have been deposited (Voltea B.V., The Netherlands). These are commercial electrodes containing approximately 300 g per square meter of film. Considering that our cell allows circular collectors with 2 cm diameter, the total mass of carbon used is 0.094 g. The cell depicted in Figure 3b can be used with different separations between electrodes. In our case, we used 1 mm for all the experiments presented. The electrodes are in contact with a supercapitor (Bootscap cell

supercapacitor, C=350 F, Maxwell Technologies, USA), that acts as the charging source, and that is also used in the discharging step through a selected load resistor. During the charging step, only the cable resistance is used as R_L ($\approx$1Ω), whereas during the discharging step, the cell is connected again to the supercapacitor through an R_D =8Ω resistor, comparable to the internal resistance of the cell filled with the river water solution at room temperature. The voltage V_{cell} between both electrodes is measured as a function of time with a Keithley 2700 (USA) bench multimeter.
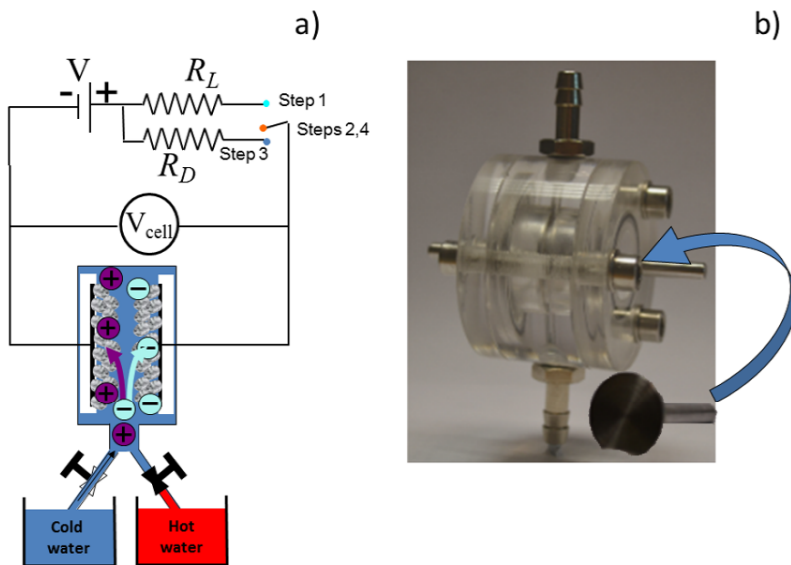
Figure 3: a) Schematic representation of the capacitive mixing cell; V_{cell} is the charging voltage, and R_L=1Ω is the resistor used for charging as external load. The resistor used for discharging in step 3 is $R_D = 8$ Ω. b) Experimental cell and electrode.

Results and discussion

Theoretical predictions

The predictions of the model are presented in Figure 4. Note how, as expected, both the surface charge density and the differential capacitance per unit area C_d decrease with temperature. It is also noticeable that the capacitance decreases with the surface potential instead

12

of increasing with it as expected, due to the fact that a larger surface potential cannot be compensated for by a larger accumulation of finite-size ions near the surface.
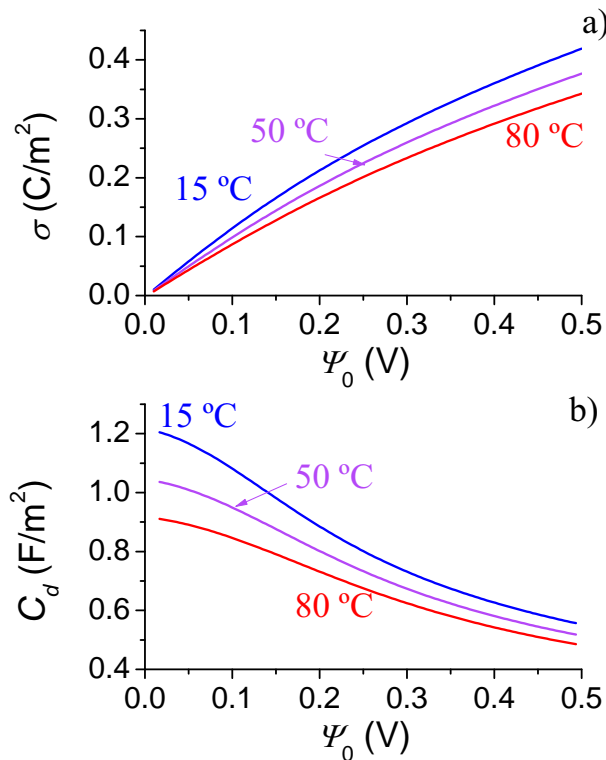

Figure 4: Surface charge density (a) and differential capacitance of the EDL (b) as a function of the surface potential for the temperatures indicated. Ionic concentration 2 M NaCl. Pore size: 5 nm. Ionic radii: Na^+ 0.36 nm and Cl^- 0.33 nm.

In Figure 5 we show the theoretical predictions for DLPE cycles as compared to CDLE ones. One important characteristic of the CDLE cycle is that the dependence of the potential jump $\Delta\Psi$ on the external charging potential reaches a plateau value for moderate electrode potentials (Figure 5a). In the case of the charge exchanged, $\Delta\sigma$, a maximum value is predicted (Figure 5b), so that beyond a given external voltage the exchanged charge and hence the extracted energy decrease, reducing the efficiency of the process,[23] as shown in Figure 5c. In[23] it was shown that the maximum extracted energy comes out as a consequence of the predicted decrease of the differential capacitance of the salty water below that of the river water, beyond a given wall potential. Such effect has the consequence of a lower exchanged charge between the electrodes. Interestingly, this is not the case with DLPE: we

13

can increase both the potential drop and the exchanged charge by increasing the electrode potential Ψ_0. We expect, hence, that at a certain potential the extracted energy in a DLPE cycle turns out to be larger than that achievable by means of the standard CDLE method (Figure 5c). From the comparison between CDLE and DLPE we can conclude that in general the salinity difference is a better technology, and that the potential advantage of the new proposal is the large availability of water with thermal gradients. In addition, it is, in principle, possible to find a working voltage above which it would be feasible to use DLPE with advantage as long as a temperature difference of about 35 °C is available.

Considering that they stem from similar principles, it will be clear that DLPE and CDLE are not incompatible. We can perform a cycle in which cold salty water is exchanged with warm river water in a sort of *CDLE+DLPE* technique. Theoretical predictions in Figure 6 confirm the advantage of this approach: we can expect to have a monotonous increase of the voltage jump, and thus, of the extracted energy with the working potential. Furthermore, the energy extracted can be up to five times larger if river water is 50 °C above sea water. Even for more realistic temperature differences (45 °C to 25 °C, say), a factor of two in the energy gain is achievable.

Experimental Results

DLPE demonstration

In Figure 7 we show an example of the voltage between electrodes in a DLPE cycle. For this example, we have used 20 mM, which is a reasonable value for the salt concentration of a typical river. The stages of Figure 2 are clearly distinguishable. In particular, the present figure demonstrates that upon exchanging cold by hot water (1→2 in Figure 7), the voltage increases. Hence, the discharge in the following step (2→3 in Figure 7) occurs at a higher potential, resulting in a positive energy balance. It can be seen that the discharging occurs in two steps. There is an initial fast decrease, due to the voltage decay between electrodes, followed by a slower decrease up to the supercapacitor value. Note that once

the external circuit is connected, conduction is allowed through the external circuit but also between electrodes through the conductive solution. Hence, special care must be taken on the selection of the load resistor used in the discharging step,[31] in order to maximize the power transfer. A note must be added concerning the possibility of generation of thermoelectric effects in the hot-water stage. If it is assumed that the cables connecting the cell to the voltmeter are 0.5 m long, and taking into account that the thermoelectric power of Cu is 4 μV/K, it can be estimated that at most 0.2 mV could be added to the voltmeter reading, but this value is about 20 times smaller than the maximum voltage measured in DLPE.

CDLE and DLPE compared

In Figure 8 succesive cycles like that in Figure 7 are shown in comparison with CDLE cycles. We can observe that the values of $\Delta\Psi$ are lower in DLPE than in CDLE cycles, for otherwise identical charging conditions. Note that because the extracted work depends on both the charge exchanged with the external voltage source and the potential jump under solution exchange, and both are lower in DLPE, we can predict a reduced extracted work with the latter technique. However, we can improve on these results, as described below.

Both techniques together

A clear way of improving on both DLPE and CDLE used separately is the use of both techniques together. Data in Figure 9 prove that optimum conditions can be found in which properly combining temperature and salinity differences makes it possible to maximize the voltage rise in the mixed CDLE+DLPE technique. If 600 mM is the concentration of the sea water and 25°C its temperature, $2\Delta\Psi$ can be as high as 80 mV if the river water (20 mM NaCl) is at 75 °C. Note however that upon increasing the salty water concentration up to 1 M the improvement is reduced and the advantage of using higher salinity is compensated for by a likely larger loss associated to the high conductivity of the solution.

In fact, the presence of charge leakage can be made clear when considering the experi-

15

mental charge-potential cycles, similar to that shown in Figure 2. From the measurement of both the current through the external load and of the cell voltage, together with the cycle duration (Figures 10a, 10b) it is possible to evaluate the charge-potential cycle, and the results are plotted in Figure 11. Note that the area of the cycle increases with the river water temperature (and so does the energy extracted, in consequence), and furthermore that in some cases, the cycles do not close properly, indicating charge losses, probably attributable to electrode redox reactions.[1]

The increase of power density obtained with river water temperature is explicitly shown in Figure 12a. Even if the temperature difference available is moderate (40-60 °C) the power can be increased by a factor of 2-4. This is a clear confirmation of the feasibility of the mixed technique in easily achieved conditions in practice. As an additional advantage, we have evaluated the energy production for increasing charging voltages. As predicted by the data in Figure 5, the energy associated to the DLPE process always increases with the charging voltage, contrary to CDLE alone, where a maximum is theoretically and experimentally found.[23,31] In contrast, the results in Figure 12b demonstrate that we can always gain power by increasing the source voltage as far as the limit imposed by faradaic reactions is not surpassed.

Data in Figure 12 show that the maximum power density that we have reached for the selected experimental conditions is 40 mW/m^2 (130 mW/kg) in CDLE+DLPE. These values must be compare to those of related technologies, where a either salinity or temperature gradients are essential ingredients. Thus, the CDP technology can reach 0.2 W/m^2,[32] and the values rises to 2.2 W/m^2 in the case of RED devices.[33] In the case of thermoelectric power generators, the reported power ranges between 1 and 10 W/kg for temperature differences of about 200 °C.[34]

In terms of the amount of water required to perform a CDLE+DLPE cycle, we estimate that the energy produced amounts to 5.4 J/l. This value is about 1/100 lower than the maximum predicted by Pattle.[35] Even so, our experimental results qualitatively confirm

16

our theoretical predictions. In order to reach a more quantitative agreement, it would be necessary to estimate the fraction of pore area that is effectively wetted and participates in the exchanging process. In fact, we have the possibility of using the experimental transferred charge as an indicative of the effective wetted area. From this, the efficiency of the process can be calculated by comparing the area of the experimental cycle with that calculated theoretically for the same charge transfer and charging voltages. The average value in the CDLE+DLPE cycle is around 30%. Losses involved in self-discharging during the open circuit stages and dissipation in the internal resistance of the cell (walls and solution) can account for this limited efficiency.

However, considering that the CDLE+DLPE technique is just starting to be implemented, it is reasonable to expect significant improvements in efficiency and power density when the technology is further developed. Improvements are expected to come from: optimum control of the duration of the different cycle stages; cell geometry; electrode material selection, concerning wettability, pore size distribution and conductivity; minimization of the charge leakage, scaling up the device maximizing the electrode area and minimizing the electrode gap in order to reduce the internal resistance.

The results just discussed show that the technique based on the dependence of the electric double layer capacitance with temperature can be used as a new approach for the extraction of electrical energy from thermal gradients without the need of electromechanical converters. It only requires electrodes with enough surface area and can be implemented wherever water or any other solvent at two temperatures and/or salinities is available. The concept is very promising and we have shown some lines along which improvements can be achieved. In addition, it can be used in combination with other well known sources of renewable energy, such as solar thermal plants, geothermal extraction, or even home solar collectors as a source of heat during the long periods of inactivity.

17

Acknowledgement

References

(1) Brogioli, D. Extracting renewable energy from a salinity difference using a capacitor. *Phys. Rev. Lett.* **2009**, *103*, 058501.

(2) Brogioli, D.; Zhao, R.; Biesheuvel, P. M. A prototype cell for extracting energy from a water salinity difference by means of double layer expansion in nanoporous carbon electrodes. *Energy Environ. Sci.* **2011**, *4*, 772–777.

(3) Bijmans, M.; Burheim, O.; Bryjak, M.; Delgado, A.; Hack, P.; Mantegazza, F.; Tenisson, S.; Hamelers, H. Capmix -deploying capacitors for salt gradient power extraction. *Energy Procedia* **2012**, *20*, 108 – 115.

(4) Sales, B. B.; Saakes, M.; Post, J. W.; Buisman, C. J. N.; Biesheuvel, P. M.; Hamelers, H. V. M. Direct power production from a water salinity difference in a membrane-modified supercapacitor flow cell. *Environ. Sci. Technol.* **2010**, *44*, 5661–5665.

(5) Sales, B. Capacitive Technology for Energy Extraction from Chemical Potential Differences (ISBN: 978-94-6173-738-0). Ph.D. thesis, Univ. Wageningen, The Netherlands, 2013.

(6) Sales, B. B.; Liu, F.; Schaetzle, O.; Buisman, C. J.; Hamelers, H. V. Electrochemical characterization of a supercapacitor flow cell for power production from salinity gradients. *Electrochim. Acta* **2012**, *86*, 298 – 304.

(7) Hunter, R. *Foundations of Colloid Science*; Oxford University Press: Oxford, 2000.

(8) Conway, B. *Electrochemical Supercapacitors: Scientific Fundamentals and Technological Applications*; Kluwer Academic: New York, 1999.

(9) Lyklema, J. In *Fundamentals of Interface and Colloid Science, vol. II: Solid-Liquid Interfaces*; Press, A., Ed.; Academic Press: New York, 1995.

(10) Merlet, C.; Rotenberg, B.; Madden, P. A.; Taberna, P.-L.; Simon, P.; Gogotsi, Y.; Salanne, M. On the molecular origin of supercapacitance in nanoporous carbon electrodes. *Nat. Mater.* **2012**, *11*, 306–310.

(11) Bazant, M. Z.; Storey, B. D.; Kornyshev, A. A. Double layer in ionic liquids: overscreening versus crowding. *Phys. Rev. Lett.* **2011**, *106*, 046102.

(12) Tanimura, A.; Kovalenko, A.; Hirata, F. Molecular theory of an electrochemical double layer in a nanoporous carbon supercapacitor. *Chem. Phys. Lett.* **2003**, *378*, 638 – 646.

(13) Rica, R. A.; Brogioli, D.; Ziano, R.; Salerno, D.; Mantegazza, F. Ions transport and adsorption mechanisms in porous electrodes during capacitive-mixing double layer expansion (cdle). *J. Phys. Chem. C* **2012**, *116*, 16934–16938.

(14) Rica, R. A.; Ziano, R.; Salerno, D.; Mantegazza, F.; Bazant, M. Z.; Brogioli, D. Electrodiffusion of ions in porous electrodes for capacitive extraction of renewable energy from salinity differences. *Electrochim. Acta* **2013**, *92*, 304 – 314.

(15) Bazant, M. Z.; Kilic, M. S.; Storey, B. D.; Ajdari, A. Towards an understanding of induced-charge electrokinetics at large applied voltages in concentrated solutions. *Adv. Colloid Interface Sci.* **2009**, *152*, 48–88.

(16) Ahualli, S.; Jiménez, M. L.; Carrique, F.; Delgado, A. V. Ac electrokinetics of concentrated suspensions of soft particles. *Langmuir* **2009**, *25*, 1986–1997.

(17) Greberg, H.; Kjellander, R. Charge inversion in electric double layers and effects of different sizes for counterions and coions. *J. Chem. Phys.* **1998**, *108*, 2940–2953.

(18) López-García, J. J.; Aranda-Rascón, M. J.; Grosse, C.; Horno, J. Equilibrium electric double layer of charged spherical colloidal particles: effect of different distances of minimum ion approach to the particle surface. *J. Phys. Chem. B* **2010**, *114*, 7548–7556.

(19) Roa, R.; Carrique, F.; Ruiz-Reina, E. Electric double layer for spherical particles in salt-free concentrated suspensions including ion size effects. *Phys. Chem. Chem. Phys.* **2011**, *13*, 3960–3968.

(20) Plischke, M.; Henderson, D. Pair correlation-functions and density profiles in the primitive model of the electric double-layer. *J. Chem. Phys.* **1988**, *88*, 2712–2718.

(21) Henstridge, M. C.; Dickinson, E. J.; Compton, R. G. On the estimation of the diffuse double layer of carbon nanotubes using classical theory: Curvature effects on the Gouy-Chapman limit. *Chem. Phys. Lett.* **2010**, *485*, 167 – 170.

(22) Goel, T.; Patra, C. N.; Ghosh, S. K.; Mukherjee, T. Effect of ionic size on the structure of cylindrical electric double layers: a systematic study by monte carlo simulations and density functional theory. *J. Phys. Chem. B* **2011**, *115*, 10903–10910.

(23) Jiménez, M.; Fernández, M.; Ahualli, S.; Iglesias, G.; Delgado, A. Predictions of the maximum energy extracted from salinity exchange inside porous electrodes. *J. Colloid Interface Sci.* **2013**, *402*, 340 – 349.

(24) Guerrero-García, G. I.; González-Tovar, E.; Lozada-Cassou, M.; Guevara-Rodríguez, F. D. The electrical double layer for a fully asymmetric electrolyte around a spherical colloid: An integral equation study. *J. Chem. Phys.* **2005**, *123*, 034703.

(25) Messina, R. Electrostatics in soft matter. *J. Phys.-Condens. Matt.* **2009**, *21*, 113102.

(26) Kilic, M. S.; Bazant, M. Z.; Ajdari, A. Steric effects in the dynamics of electrolytes at large applied voltages. I. Double-layer charging. *Phys. Rev. E* **2007**, *75*, 021502.

(27) Biesheuvel, P. M.; van Soestbergen, M. Counterion volume effects in mixed electrical double layers. *J. Colloid Interface Sci.* **2007**, *316*, 490–499.

(28) Adamczyk, Z.; Warszynski, P. Role of electrostatic interactions in particle adsorption. *Adv. Colloid Interface Sci.* **1996**, *63*, 41–149.

(29) Borukhov, I. Charge renormalization of cylinders and spheres: Ion size effects. *J. Polymer Sci. Part B-Polymer Phys.* **2004**, *42*, 3598–3615.

(30) Bockris, J.; Reddy, A. In *Modern Electrochemistry*; Plenum,, Ed.; Plenum: New York, 1970.

(31) Iglesias, G. R.; Fernández, M. M.; Ahualli, S.; Jiménez, M. L.; Kozynchenko, O. P.; Delgado, A. V. Materials selection for optimum energy production by double layer expansion methods. *J. Power Sources* **2014**, *261*, 371 – 377.

(32) Liu, F.; Schaetzle, O.; Sales, B. B.; Saakes, M.; Buisman, C. J. N.; Hamelers, H. V. M. Effect of additional charging and current density on the performance of Capacitive energy extraction based on Donnan Potential. *Energy Environ. Sci* **2012**, *5*, 8642–8650.

(33) Vermaas, D. A.; Saakes, M.; Nijmeijer, K. Doubled Power Density from Salinity Gradients at Reduced Intermembrane Distance. *Environ. Sci. Technol.* **2011**, *45*, 7089–7095.

(34) Crane, D.; Lagrandeur, J.; Harris, F.; Bell, L. Performance Results of a High Power-Density Thermoelectric Generator: Beyond the Couple. *J Electron Mater* **2009**, *38*, 1375–1381.

(35) Pattle, R. E. Production of electric power by mixing fresh and salt water in the hydro-electric pile. *Nature* **1954**, *174*, 660–660.
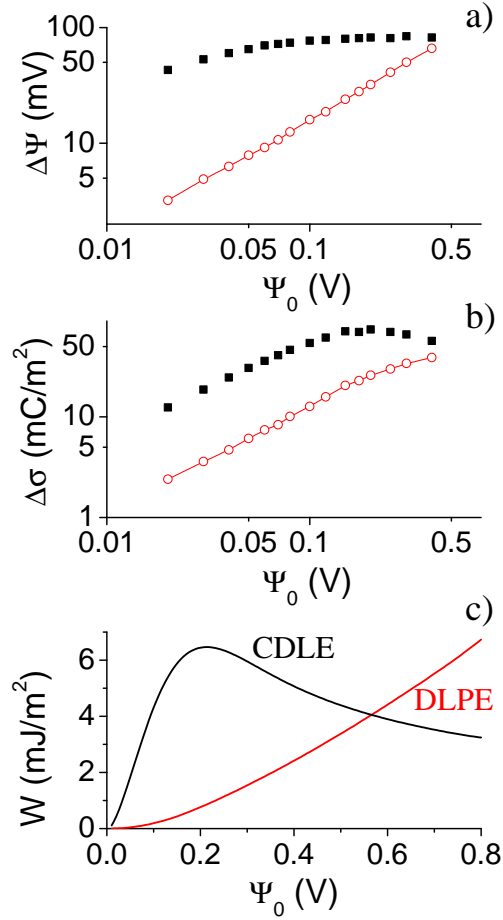
Figure 5: Theoretical results of a) potential jump in step 1→2, that is, when the cell capacitance changes from high to low by means of either salinity (CDLE, full squares) or temperature (DLPE, open circles) variations. b) Surface charge density exchanged between the external battery and the electrodes in step 2→3 (Figure 2). c) Extracted work as a function of the potential difference between the electrode and the solution. Pore size: 5 nm. In DLPE: NaCl concentration: 0.5 M, temperatures 15 °C and 50 °C; in CDLE: temperature 15 °C, NaCl concentrations: 0.02 mM and 0.5 M.
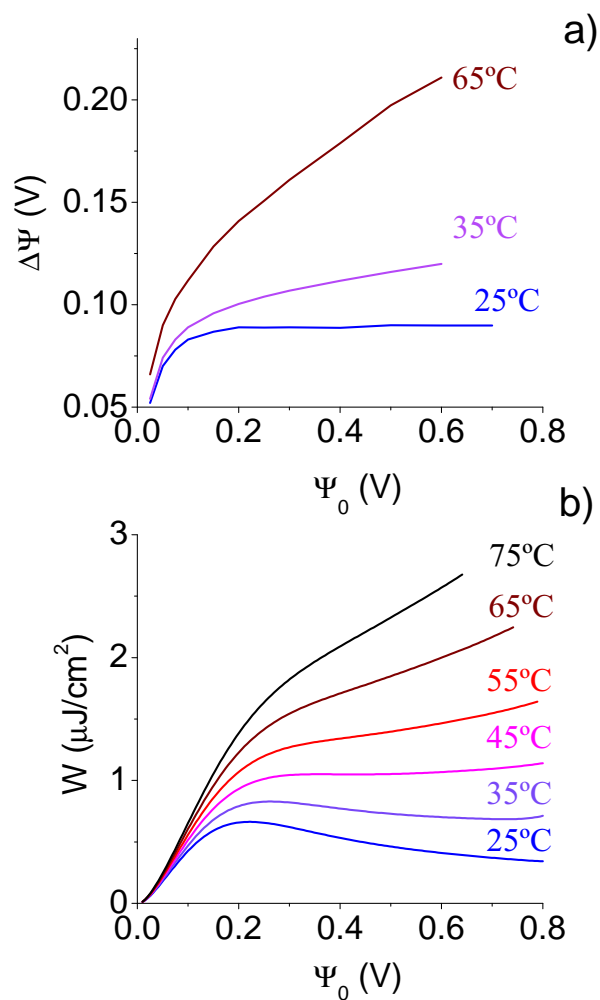
Figure 6: Theoretical results of the potential rise $\Delta\Psi$ (a) and extracted energy per unit interfacial area in CDLE+DLPE cycles (b) as a function of the electrode potential Ψ_0. Sea water in all cases: 25 °C. The temperature of the river water is indicated. Pore size: 5 nm. Sea water 0.5 M NaCl; River water: 0.02 M NaCl.
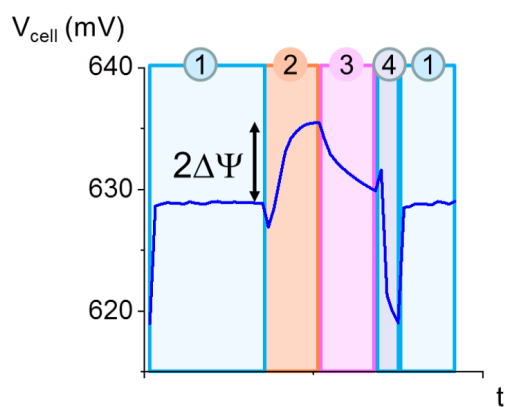
Figure 7: Experimental results of the cell potential, V_{cell}, as a function of time during a DLPE cycle. Cold water: 25 °C, hot water: 50 °C. NaCl concentration 20 mM. $|\Delta\Psi|$ is the voltage jump in each electrode.
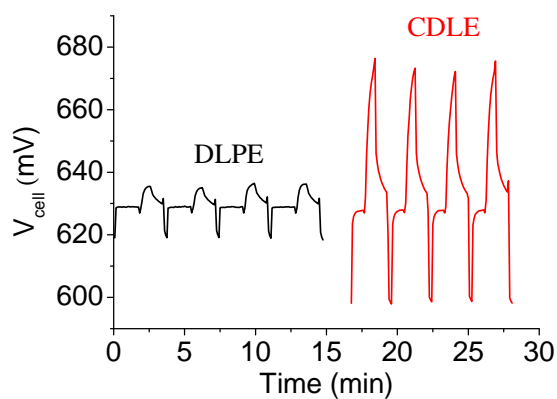
Figure 8: Experimental results of the potential as a function of time during succesive cycles of DLPE (black) and CDLE (red). Charging voltage $V = 630$ mV; solution used in DLPE: 20 mM NaCl at 25 °C and 50 °C; exchanged solutions in CDLE: 20 and 600 mM NaCl at 25 °C .
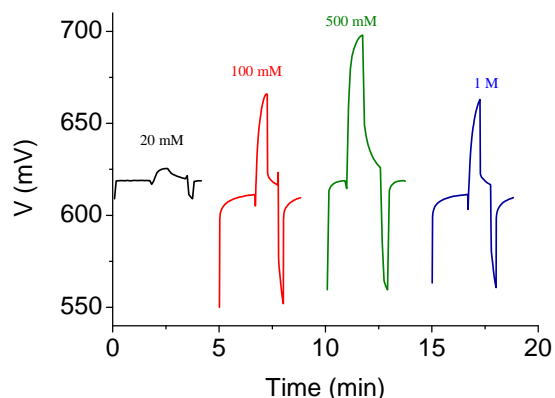
Figure 9: Experimental voltage between electrodes as function of time for CDLE-TG cycles in which a 20 mM NaCl solution at 75 °C is inside the cell during the discharging step while the charging steps are performed with a solution of the concentration indicated and at at 25 °C.
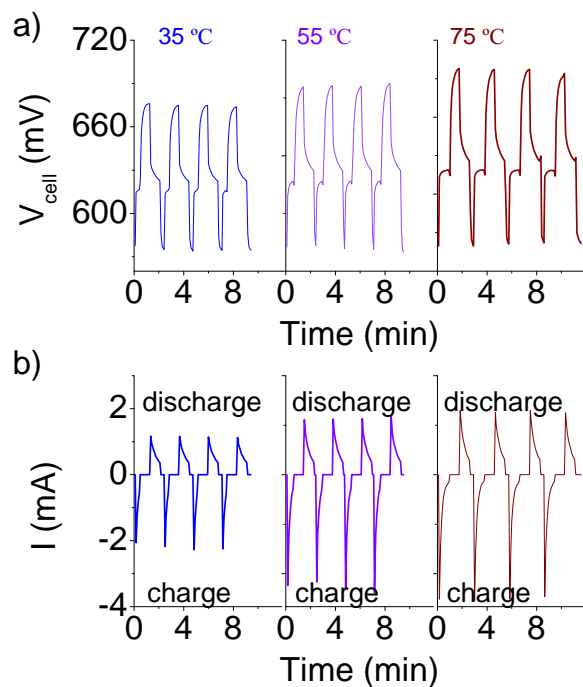

Figure 10: Experimental cell voltage (a) and electric current through the cell (b) as a function of time for CDLE+DLPE cycles in which a 20 mM NaCl solution is inside the cell during the discharging step and at the temperatures indicated. In all cases, the charging step is performed with a 600 mM solution at 25°C.
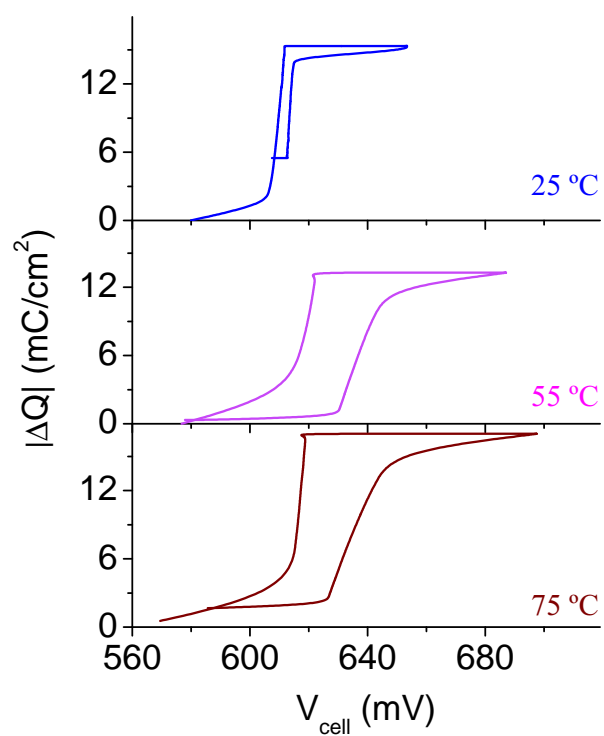
Figure 11: Experimental ΔQ -V_{cell} cycles for CDLE (25 °C-25 °C) and CDLE+DLPE (25 °C-55 °C and 25 °C-75 °C).
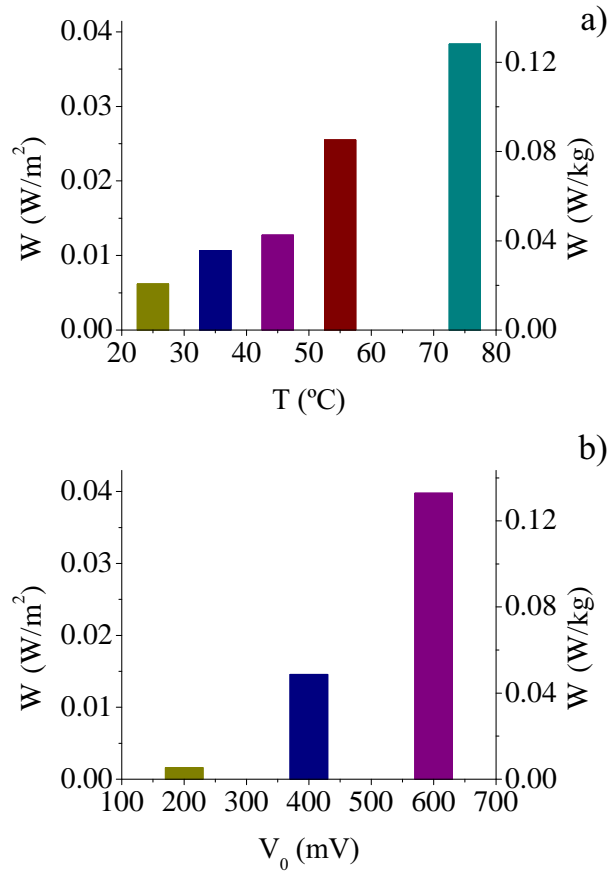
Figure 12: Experimental values of the extracted energy per unit apparent surface area of elctrode for CDLE+DLPE cycles. a) Charging solution: NaCl 600 mM at 25°C; discharging solutions: NaCl 20 mM at the indicated temperatures and 620 mV charging voltage. b) Charging solution as in a) and discharging solution: NaCl 20 mM at 75°C, for the indicated charging voltages.